

Review of the Major and Minor Salivary Glands, Part 2: Neoplasms and Tumor-like Lesions

Alexander T Kessler, Alok A Bhatt

Department of Imaging Sciences, University of Rochester Medical Center, Rochester, New York, USA



Received : 16-06-2018
Accepted : 06-10-2018
Published : 15-11-2018

ABSTRACT

The salivary glands are small structures in the head and neck, but can give rise to a wide variety of benign and malignant pathology. When this occurs, patients may present with palpable swelling, although it is quite common that they are asymptomatic and a salivary gland mass was discovered as an incidental finding on imaging performed for another reason. It is, therefore, critical that radiologists pay careful attention to the salivary glands and have working knowledge of the key differentiating features of the most common neoplastic and nonneoplastic etiologies of salivary gland masses. The purpose of this review is to provide a succinct image-rich article illustrating the various causes of salivary gland masses via an extensive review of the primary literature. In Part 2, we discuss neoplasms and tumor-like lesions of the salivary glands with a key emphasis on specific imaging features of the most common pathologic entities.

KEYWORDS: *Ranula, salivary gland neoplasms, salivary glands, vascular malformations*

INTRODUCTION

Salivary gland neoplasms constitute a wide variety of benign and malignant tumors, most recently delineated in the WHO Classification of Salivary Gland Tumors in 2005.^[1] Review of this classification demonstrates that there are >40 possible neoplasms that can arise in the salivary glands. This has become the source of much apprehension among radiologists, as many of these salivary gland neoplasms share similar appearances on imaging. Fortunately, the superficial location of the salivary glands makes tissue sampling relatively easy to perform, obviating the need for accurate radiologic diagnosis. That being said, knowledge of epidemiology and key imaging characteristics of the most common salivary gland neoplasms can help radiologists limit the differential and make more accurate presurgical diagnostic predictions. We first discuss imaging techniques as well as review several common salivary gland neoplasms focusing on key radiologic characteristics that may help the reader make specific imaging diagnoses. This will be followed by a review of common nonneoplastic tumor-like lesions frequently encountered in the salivary glands.

SALIVARY GLAND IMAGING TECHNIQUES

Before discussing salivary gland lesions, it is important to review the strengths and weaknesses of the various imaging modalities available. Conventionally, radiography and sialography were the workhorse of salivary gland imaging due to their ability to detect calcifications and exquisitely visualize the ductal system. Although sialography is still used for certain indications (i.e., identifying sialoliths or dilating strictures in cases of chronic sialadenitis), these modalities cannot adequately visualize the vast majority of salivary gland neoplasms and have largely been replaced by cross-sectional imaging, namely ultrasound, computed tomography (CT), and magnetic resonance imaging (MRI).

Ultrasound is a quick and relatively inexpensive modality that can accurately depict the vast majority of salivary gland

Address for correspondence: Dr. Alexander T Kessler, 601 Elmwood Avenue, Box 648, Rochester, New York 14642, USA. E-mail: atkessler8@gmail.com

This is an open access journal, and articles are distributed under the terms of the Creative Commons Attribution-NonCommercial-ShareAlike 4.0 License, which allows others to remix, tweak, and build upon the work non-commercially, as long as appropriate credit is given and the new creations are licensed under the identical terms.

For reprints contact: reprints@medknow.com

How to cite this article: Kessler AT, Bhatt AA. Review of the Major and Minor Salivary Glands, Part 2: Neoplasms and Tumor-like Lesions. J Clin Imaging Sci 2018;8:48. Available FREE in open access from: <http://www.clinicalimagingscience.org/text.asp?2018/8/1/48/245528>

Access this article online	
Quick Response Code: 	Website: www.clinicalimagingscience.org
	DOI: 10.4103/jcis.JCIS_46_18

neoplasms. Due to their superficial location, the margins of most salivary gland neoplasms can be delineated through the use of high-frequency transducers (7–10 MHz). This allows the radiologist to not only determine the size of the lesion but also help guide the site of biopsy/aspiration, especially in cases where a lesion demonstrates mixed cystic/solid components. However, as with all modalities, ultrasound carries significant limitations. It is heavily operator dependent, provides limited visualization of the deep lobe of the parotid gland, and often has difficulty distinguishing benign from malignant neoplasms. It is for these reasons that ultrasound is not commonly used unless there is limited access to other advanced imaging techniques such as CT or MRI.

CT is frequently the first test to identify a salivary gland lesion due to the fact that many lesions are often incidentally discovered on CT performed for other reasons. Compared to other cross-sectional imaging, CT is an extremely fast imaging technique, but carries the risk of ionizing radiation. CT is very good at identifying salivary gland lesions, but is particularly useful for identifying lesions with calcifications (i.e., phleboliths in venous malformations). However, due to relatively poor soft-tissue contrast, defining tumor extent and attempting to differentiate benign from malignant neoplasms can be quite challenging.

MRI is currently the test of choice in evaluating salivary gland lesions. Not only can it identify and properly size most lesions, but its higher soft tissue resolution allows for better identification of internal tumor characteristics, better definition of tumor margins, and most importantly, identification of perineural spread. In addition, advanced MRI techniques such as diffusion-weighted imaging (DWI) have proven helpful in better characterizing various lesions (i.e., identifying malignant transformation of a pleomorphic adenoma as areas of low apparent diffusion coefficient [ADC] signal in an otherwise hyperintense mass).

SALIVARY GLAND NEOPLASMS

When faced with a newly discovered salivary gland mass, it is imperative that the radiologist understands the basic morphologic differences between benign and malignant salivary tumors. Small benign neoplasms (<2 cm) are typically well circumscribed and demonstrate either minimal enhancement (Warthin's tumor) or homogeneous enhancement (pleomorphic adenoma). Large benign neoplasms (>2 cm) are typically well circumscribed, but often show heterogeneous enhancement as they outgrow their blood supply. Low-grade malignant neoplasms tend to mimic benign neoplasms in that they are often well circumscribed, but may show varying degrees of enhancement. High-grade

malignant neoplasms, on the other hand, have infiltrative margins and often have nodal metastases or perineural spread at the time of diagnosis.

It is also important that the radiologist should be aware of the reported incidence of the most common salivary gland tumors.^[2] In the parotid gland, approximately 80% of neoplasms are benign while 20% are malignant. The most common benign parotid gland neoplasms are pleomorphic adenoma and Warthin's tumor while the most common malignant neoplasm is mucoepidermoid carcinoma. In the submandibular gland, 50% of neoplasms are benign while 50% are malignant. As in the parotid gland, the most common benign neoplasm is the pleomorphic adenoma, constituting 85% of all benign submandibular gland neoplasms. The most common malignant neoplasms include adenoid cystic carcinoma (ACC), mucoepidermoid carcinoma, and the malignant mixed tumors (a diverse group of tumors predominantly consisting of carcinosarcoma and carcinoma ex pleomorphic adenoma). In the sublingual and minor salivary glands, 80%–90% of neoplasms are malignant. ACC is the most common, while mucoepidermoid carcinoma is the second most common, with these two tumors comprising the overwhelming majority of all neoplasms.

Although the imaging appearance of a salivary gland mass is often nonspecific, combining this statistical knowledge with the previously described imaging characteristics can allow the radiologist to favor a benign or malignant process, as well as suggest the most common pathologic considerations. In addition, review of the literature shows that many salivary gland neoplasms have specific imaging features, that if identified, can significantly raise the confidence of the reader to suggest a particular diagnosis. What follows is a discussion of common salivary gland neoplasms with emphasis on key imaging features of each pathologic entity [Table 1].

PLEOMORPHIC ADENOMA

Pleomorphic adenoma (benign mixed tumor) is a neoplasm comprised a combination of glandular epithelium and myoepithelial components. It is the most common benign salivary gland neoplasm and has a female predominance (2:1), typically affecting patients aged 30–60 years. Nearly 80% of these lesions arise in the parotid gland, and of these, 80%–90% arise in the superficial portion of the gland.^[3–5] On imaging, pleomorphic adenomas can have a variety of imaging appearances owing to their variable histologic makeup. However, the classic imaging appearance is that of a well-circumscribed multilobulated mass with high T2/ADC signal, greater than cerebrospinal fluid signal [Figure 1]. In fact, Zaghi et al., suggested that

if a mass demonstrates bright T2 signal, sharp margins, heterogeneous nodular enhancement, lobulated contours, and a dark T2 rim, this combination of features carries 95% specificity for pleomorphic adenoma.^[6]

CARCINOMA EX PLEOMORPHIC ADENOMA

Carcinoma ex pleomorphic adenoma refers to malignant transformation of a preexisting pleomorphic adenoma. Although rare, it has been reported to occur in 0.15% of lesions.^[7] On imaging, new infiltrative margins and rapid enlargement of a preexisting well-circumscribed salivary gland mass are features, highly suggestive of transformation [Figure 2]. Some authors suggest that DWI and ADC maps can be helpful in identifying areas of malignant transformation as areas of carcinoma are

typically hypercellular and therefore demonstrate high DWI and low ADC signal. However, these same authors point out that using DWI alone can be problematic as necrosis is commonly seen with these carcinomas, producing areas of hypocellularity and therefore a false negative imaging appearance.^[8]

WARTHIN’S TUMOR

Warthin’s tumor (papillary cystadenoma lymphomatosum) is a benign neoplasm comprised both epithelial and

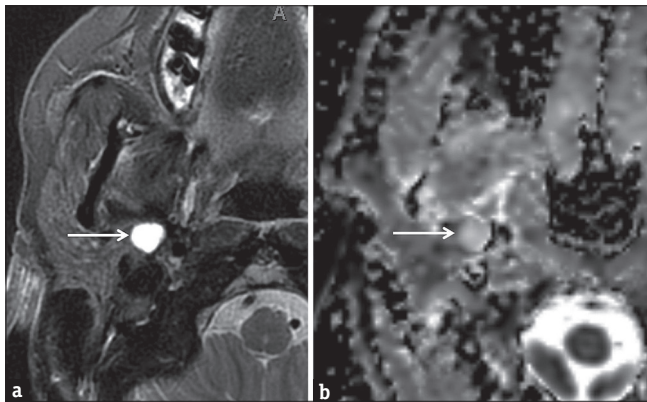


Figure 1: Pleomorphic adenoma. Axial T2-weighted (a) and axial apparent diffusion coefficient (b) Magnetic resonance images demonstrate a well-circumscribed high signal lesion in the deep portion of the right parotid gland (white arrows). Note that the lesion demonstrates T2 hyperintensity greater than nearby cerebrospinal fluid.

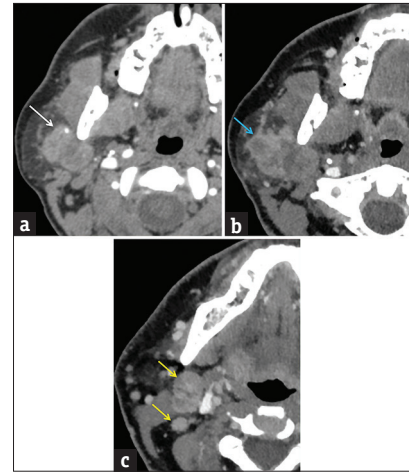


Figure 2: Carcinoma ex pleomorphic adenoma. (a) Axial computed tomography image demonstrates a well-circumscribed mass spanning the superficial and deep portions of the right parotid gland (red arrow), nonspecific in etiology. (b) Axial computed tomography image performed 4 months later demonstrates rapid enlargement with infiltrative margins (blue arrow). (c) Axial computed tomography image at a slightly lower level demonstrates new right level II lymph nodes (yellow arrows). Pathologically confirmed carcinoma ex pleomorphic adenoma with metastatic lymphadenopathy.

Table 1: Key imaging characteristics of salivary gland neoplasms and tumor-like lesions

	Key imaging characteristic
Neoplasm	
Pleomorphic adenoma	Bright T2 signal, sharp margins, heterogeneous nodular enhancement, lobulated contours, and dark T2 rim
Carcinoma ex pleomorphic adenoma	New infiltrative margins and rapid enlargement of a preexisting well-circumscribed salivary gland mass
Warthin’s tumor	Hypercellular microcysts, multifocal (20%).
Mucoepidermoid carcinoma	Partially cystic mass with ill-defined margins
Adenoid cystic carcinoma	Perineural spread and local invasion
Oncocytoma	Vanishing mass on T2WI and T1+C, FDG avid
Lipoma	Fat attenuation on CT, fat suppression on MRI
Intraparotid metastasis	Parotid tail or pretragal mass with primary malignancy of the ocular adnexa or cutaneous forehead and lateral aspect of the head
Hemangioma (hemangioendothelioma)	Infant, T2 hyperintense, homogeneously enhancing
Tumor-like lesion	
Ranula	T2 hyperintense lesion in the sublingual space
Venous malformation	T2 hyperintensity, gradual enhancement, phleboliths
Lymphatic malformation	Transspatial, hemorrhage-fluid levels
Arteriovenous malformation	Clustered nidus, arterial feeder, draining vein

CT: Computed tomography, MRI: Magnetic resonance imaging, FDG: Fluorodeoxyglucose

lymphoid tissue that forms papillary projections on histology. It is the second most common benign salivary neoplasm and has a strong association with smoking.^[9] Warthin's tumors most commonly arise from the parotid tail and 30% demonstrate mixed cystic and solid components. Unlike other benign salivary neoplasms such as pleomorphic adenoma, the solid components typically demonstrate minimal enhancement on postcontrast imaging. However, a more specific imaging appearance is that of hypercellular microcysts. Although not seen in all cases, identification of these microcysts within a parotid lesion is very suggestive of Warthin's tumor. On MRI, these highly cellular components correspond to areas of T1 hyperintensity, T2 hypointensity, short-tau inversion recovery (STIR) hypointensity, and low ADC signal.^[10] Although only a small percentage are bilateral or multifocal at the time of diagnosis (up to 20% of cases), they are the most common etiology of multiple intraparotid masses [Figure 3].^[11]

MUCOEPIDERMOID CARCINOMA

Mucoepidermoid carcinoma is a malignant neoplasm comprised of epidermoid and mucus-secreting epithelial cells. It is the most common malignant neoplasm of the salivary glands, and 60% of lesions arise in the parotid gland. On imaging, these tumors often have a cystic component due to their mucin content, but are otherwise quite variable in appearance. High-grade tumors classically have ill-defined margins [Figure 4].^[12] From a clinical perspective, it is important to note that the cystic quality of these lesions often results in misdiagnosis after fine-needle aspiration (FNA) due to failure to obtain diagnostic material. In these cases, a strong radiologic suspicion for mucoepidermoid carcinoma should prompt repeat FNA or excisional biopsy.^[13]

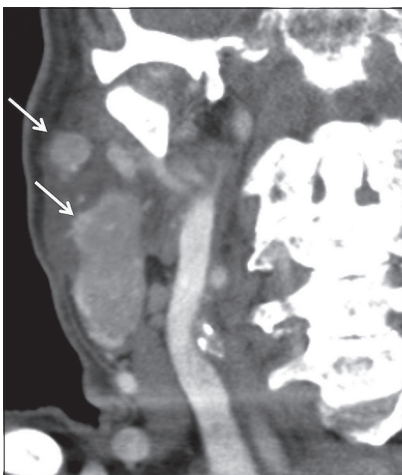


Figure 3: Warthin's Tumor. A 94-year-old male with right neck swelling. Coronal contrast-enhanced computed tomography images demonstrate multifocal enhancing masses in the right parotid gland (white arrows), pathologically proven Warthin's Tumor.

ADENOID CYSTIC CARCINOMA

ACC is a malignant neoplasm derived from both ductal and myoepithelial cells. Histologically, ACC demonstrates a mixture of three major growth patterns consisting of tubular, cribriform, and solid types. Of these, cribriform is the most common type while the solid type carries an increased risk of nodal metastasis and with it a poorer prognosis.^[14] Clinically, these patients tend to present at an older age (5th–7th decades), and of all the salivary gland tumors, ACC has the greatest propensity for perineural spread and local invasion. Despite the histologic makeup of a given lesion, ACC tends to be very aggressive and it is reported that 90% of cases will have cervical lymph node metastases at the time of diagnosis.^[15] Because of this, ACC is quite prone to late local recurrence, sometimes manifesting up to 20 years after initial diagnosis. On imaging, ACC commonly presents as an ill-defined mass with perineural spread.^[16-19] The most common single site of origin for ACC is the parotid gland (25%), often demonstrating perineural involvement of cranial nerve VII at the time of diagnosis. However, collectively the minor salivary glands constitute the majority of ACCs (60%), often with associated perineural tumor spread into the skull base [Figures 5 and 6].^[20]

ACINIC CELL CARCINOMA

Acinic cell carcinoma is a malignant neoplasm derived from the glandular epithelium and is considered a variant of adenocarcinoma. Nearly 90% of lesions arise in the parotid, most commonly located in the parotid tail.^[21] On imaging, acinic cell carcinoma typically presents as a well-circumscribed, homogeneously enhancing, slow-growing mass, similar to other benign or low-grade malignant tumors. Therefore, imaging is quite nonspecific and tissue sampling is often necessary

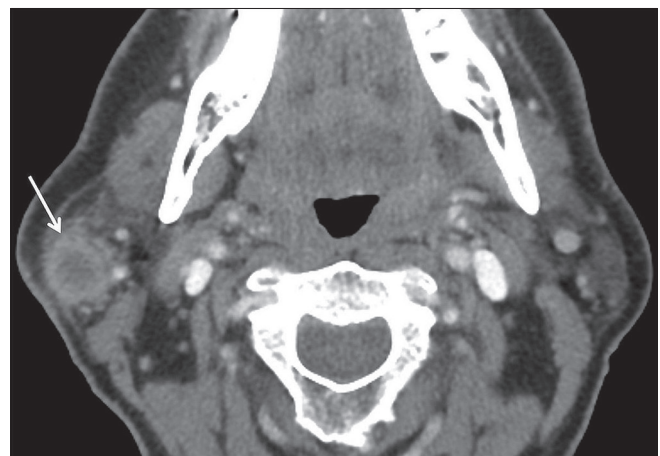


Figure 4: Mucoepidermoid Carcinoma. A 53-year-old male with right neck pain and palpable lump. Axial contrast-enhanced computed tomography image demonstrates an enhancing mass with ill-defined margins and central cystic component (white arrow).

to establish the diagnosis. As with other malignancies, acinic cell carcinoma may sometimes have a more aggressive appearance, mimicking mucoepidermoid carcinoma or ACC. In these cases, careful evaluation for spread of disease is essential [Figure 7].^[22]

ONCOCYTOMA

Oncocytoma is a benign neoplasm derived from mitochondria-rich epithelial cells. Although not

very common, these tumors have a distinct imaging appearance consisting of a lesion isointense to native salivary gland tissue on T2WI and T1+C images, producing the so-called “vanishing parotid mass.”^[23] Fluorodeoxyglucose positron emission tomography (FDG PET) can be helpful for confirmation as these lesions will demonstrate high FDG uptake due to the high content of metabolically active mitochondria [Figure 8].^[24]

LIPOMA

Lipomas are benign neoplasms composed of mature adipose tissue surrounded by a fibrous capsule. In the head and neck, they are most commonly seen near the neck base and are usually located intramuscular or within the subcutaneous fat. Salivary gland lipomas

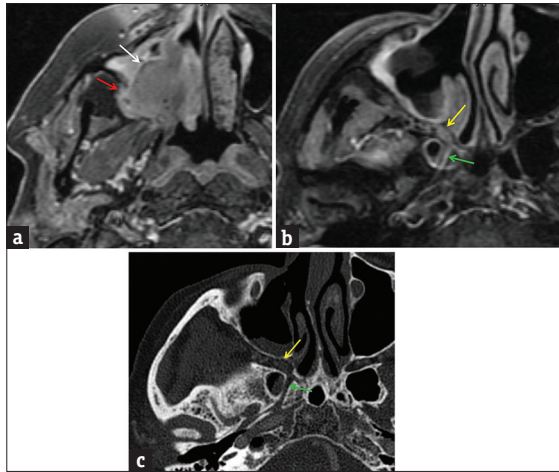


Figure 5: Adenoid cystic carcinoma, sinonasal minor salivary gland origin. (a) Axial T1-weighted postcontrast fat-suppressed magnetic resonance image demonstrates a heterogeneous mass in the right maxillary sinus (white arrow). Posteriorly, there is osseous invasion through the wall of the maxillary sinus into the retroantral fat (red arrow). Axial T1-weighted postcontrast fat-suppressed magnetic resonance image (b) and axial computed tomography image (c) demonstrate asymmetric widening and enhancement in the pterygopalatine fossa (yellow arrow) and vidian canal (green arrow), consistent with perineural spread of tumor.

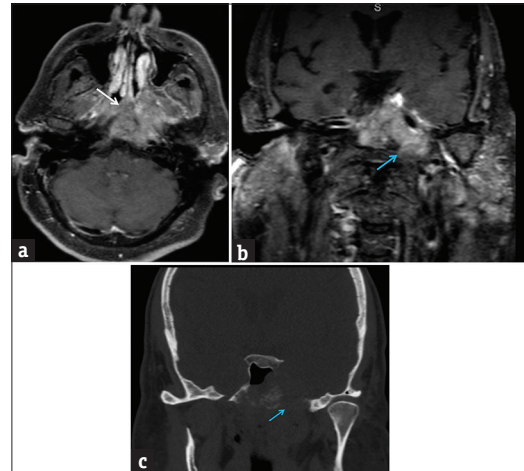


Figure 6: Adenoid cystic carcinoma, nasopharynx minor salivary gland origin. (a) Axial T1-weighted postcontrast fat-suppressed magnetic resonance image demonstrates a large heterogeneous mass centered in the nasopharynx (white arrow). Coronal T1-weighted postcontrast fat-suppressed magnetic resonance image (b) and coronal computed tomography image (c) demonstrate associated destruction of the central skull base with perineural extension through left foramen ovale (blue arrows).

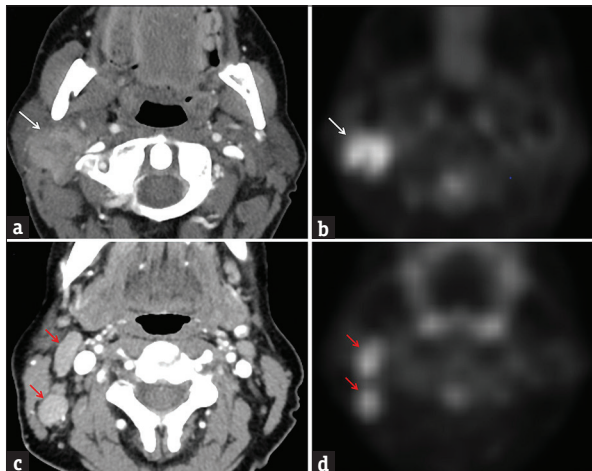


Figure 7: Acinic cell carcinoma. A 51-year-old female with enlarging palpable right parotid mass over 3 months. Axial contrast-enhanced computed tomography (a) and transverse FDG-PET (b) images demonstrate a hypermetabolic ill-defined mass within the lower right parotid gland, extending toward the tail (white arrows). At a slightly lower level, axial contrast-enhanced computed tomography (c) and transverse FDG-PET (d) images demonstrate enlarged hypermetabolic right level II lymph nodes (red arrows). Pathologically proven acinic cell carcinoma with metastatic lymphadenopathy.

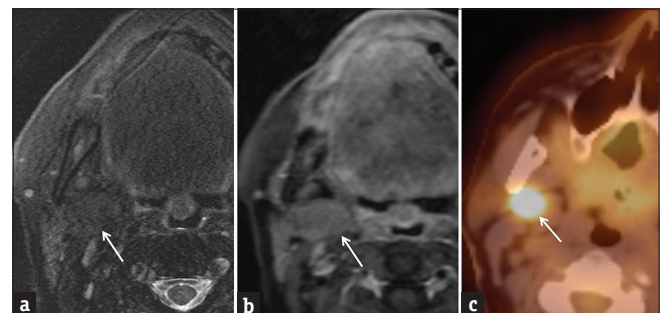


Figure 8: Oncocytoma. (a) Axial T2-weighted fat-suppressed image demonstrates a barely perceptible mass in the deep portion of the parotid gland (white arrow), isointense to normal parotid parenchyma. (b) Axial T1-weighted postcontrast fat-suppressed image also demonstrates a subtle mass isointense to normal parotid parenchyma (white arrow). (c) Transverse fused PET/computed tomography image demonstrates an obvious hypermetabolic mass (white arrow). Pathologically proven oncocytoma.

are much rarer and most commonly involve the parotid gland. They may be located with the gland itself or extracapsular within the adjacent parotid space.^[25] On imaging, there is typically no diagnostic dilemma as they will appear as well-circumscribed lesions with imaging appearance similar to fat. On CT, they will demonstrate attenuation of approximately -60 to -120 HU [Figure 9]. On MRI, they will demonstrate T1 and T2 hyperintensity and will become hypointense with fat-suppression techniques. Important to note is the rare variant sialolipoma, in which a lipoma undergoes secondary entrapment of normal salivary gland tissue. This alters the appearance of the lesion on imaging, producing a fatty lesion with heterogeneous internal composition owing to incorporation of salivary tissue.^[26] Although this may be confusing at first, any well-encapsulated heterogeneous lesion with clear fatty components should raise the suspicion for sialolipoma.

METASTATIC DISEASE

Metastatic involvement of the salivary glands is relatively rare, but most commonly seen in the parotid gland. Although many malignancies have been implicated, metastasis is typically due to cutaneous squamous cell carcinoma and melanoma.^[27] The major mechanism through which this occurs is via lymphatic spread into intraparotid lymph nodes. The presence of lymphatic tissue within the parotid gland is a unique feature among the salivary glands and occurs due to the fact that late encapsulation of the parotid gland during embryogenesis results in the incorporation of lymphoid tissue. Intraparotid lymph nodes act as the major drainage pathway of the ocular adnexa as well as the cutaneous surfaces of the forehead and lateral aspect of the head.^[28] Therefore, identification of abnormal-appearing intraparotid lymph nodes should warrant close inspection

of these regions for a primary malignancy. On imaging, metastases to intraparotid lymph nodes appear similar to metastatic lymph nodes elsewhere in the head and neck. Progressive enlargement, central necrosis, and ill-defined margins are all imaging features, suggestive of lymphatic metastasis [Figure 10]. In clinical practice, differentiating metastatic intraparotid lymph nodes from primary salivary malignancy can be extremely difficult and biopsy is often necessary. That being said, a case series by Kashiwagi et al., demonstrated that metastatic involvement most commonly involves the parotid tail and pretragal region of the superficial parotid lobe.^[28] Therefore, identification of a lesion in one of these areas in a patient with known cutaneous squamous cell carcinoma or melanoma should raise the suspicion for metastatic involvement.

HEMANGIOMA

Hemangiomas, also known as hemangioendotheliomas, are vascular lesions due to an abnormal proliferation of endothelial cells. It is the most common parotid tumor of childhood and tends to have a female predominance (3:1).^[29] Clinically, these patients usually present at 4 months of age with a rapidly growing mass that may have an overlying red/blue cutaneous lesion. Spontaneous regression is often seen after 18 months, although if large enough, surgery or sclerotherapy may be needed.^[30] MRI is extremely accurate in diagnosing these lesions as they classically appear as lobulated masses with T2 hyperintensity and homogeneous enhancement [Figure 11]. It is important to note that the vascular nature of these lesions places them at greater risk of hemorrhage during biopsy. Therefore, many authors portend that biopsy should not be performed when the MRI demonstrates features suggestive of a hemangioma.^[31]



Figure 9: Lipoma. An 81-year-old female presents with dysarthria and aphasia. Axial computed tomography image demonstrates an incidental mass in the left parotid gland with attenuation characteristics equal to fat (white arrow). Findings compatible with a parotid gland lipoma.

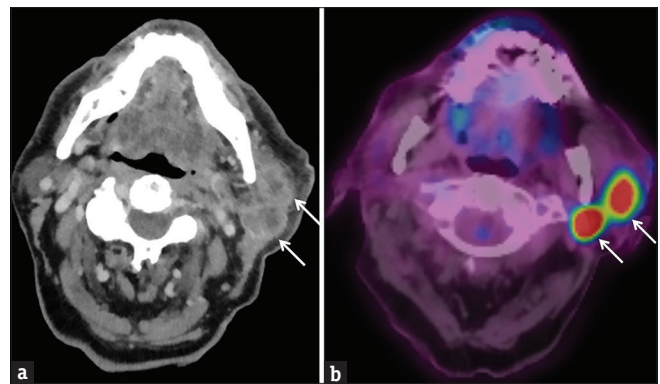


Figure 10: Intraparotid Metastases. A 90-year-old male with a history of left temple cutaneous squamous cell carcinoma presents with the left cheek swelling. Axial computed tomography (a) and fused PET/computed tomography (b) images demonstrate two hypermetabolic necrotic lymph nodes in the left parotid tail (white arrows). Biopsy-proven metastatic squamous cell carcinoma.

TUMOR-LIKE LESIONS

A variety of nonneoplastic pathologic processes may result in the imaging appearance of a salivary gland mass. It is beyond the scope of this article to discuss all of these etiologies; however, what follows is a review of the two most common nonneoplastic lesions that can be identified: ranula and vascular malformations. In addition, many infectious/inflammatory processes, such as sialadenitis and lymphoepithelial cysts, can sometimes result in the appearance of salivary gland masses and we refer you to Part 1 for further discussion.

RANULA

Ranula is defined as a mucus retention cyst or mucocele in the sublingual space arising from either the sublingual gland or the minor salivary gland tissue. Common etiologies include prior inflammation, trauma, or rarely congenital. On imaging, ranulas demonstrate homogeneous high T2 signal due to their cystic nature, but may show peripheral enhancement or internal diffusion restriction if superinfected. The term simple ranula is used when the lesion is confined to the sublingual space [Figure 12]. The term diving/plunging ranula is used when the lesion ruptures out of the sublingual space. This most commonly occurs posterolaterally into the submandibular space where the lesion has room to expand leaving behind what looks like a narrower “tail” in the sublingual space [Figure 13].^[32]

VASCULAR MALFORMATIONS

Vascular malformations constitute a diverse group of lesions that result from errors in vessel morphogenesis. Although these lesions do not demonstrate true cellular proliferation-like hemangiomas, they may grow rapidly during times of hormonal stimulation, hemorrhage, or infection.^[33] In the head and neck, vascular malformations can arise directly from the salivary tissue; however, in clinical practice, they are more commonly transspatial involving both salivary and surrounding soft tissue. In 2014, the International Society for the Study of Vascular Anomalies released an updated classification separating the malformations into the following categories: capillary, lymphatic, venous, arteriovenous, or combined.^[34] In clinical practice, many of these lesions demonstrate combined components; however, one or two dominant components can usually be identified [Figure 14]. Of these subtypes, venous, lymphatic, and arteriovenous have specific features that can be seen on imaging. Venous malformations classically demonstrate T2 hyperintensity and tend to enhance gradually on dynamic imaging. They may also contain calcified phleboliths, a feature very suggestive

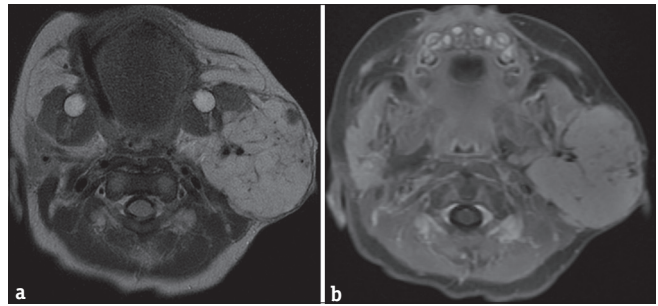


Figure 11: Hemangioma. A 1-month-old infant with left neck mass. Axial T2-weighted image (a) and axial T1-weighted postcontrast fat-suppressed (b) images demonstrate a lobulated mass in the left parotid gland with T2 hyperintensity and homogeneous enhancement, compatible with an infantile hemangioma.

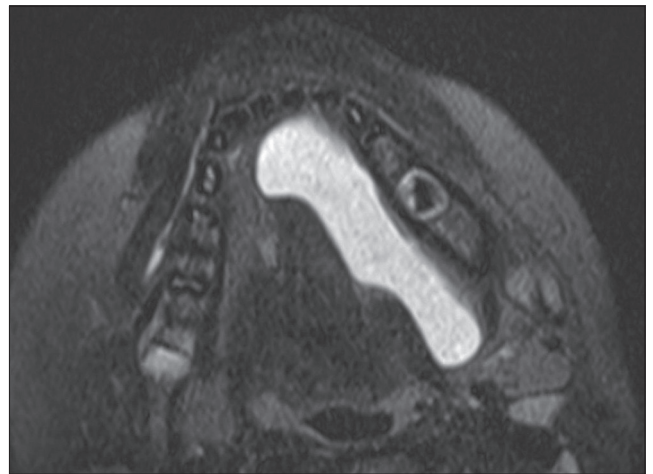


Figure 12: Simple ranula. A 7-year-old male with swelling along the left floor of mouth. Axial T2 fat-suppressed image demonstrates a cystic lesion occupying the entire left sublingual space. Note there is no extension beyond the mylohyoid sling into the submandibular space.

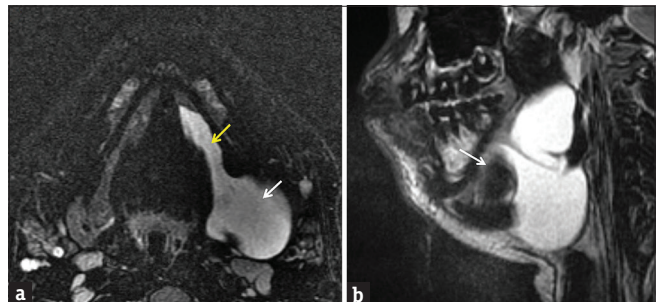


Figure 13: Plunging ranula. A 15-year-old male with swelling along the left floor of the mouth. Axial (a) and sagittal (b) T2-weighted fat-suppressed images demonstrate a cystic lesion occupying the entire sublingual space with extension beyond the posterior margin of the mylohyoid sling (white arrow) into the submandibular space. Note narrower “tail” (yellow arrow) in the portion left behind in the sublingual space.

of a venous component. Lymphatic malformations tend to be more transspatial than their venous counterpart and classically demonstrate hemorrhage-fluid levels. Arteriovenous malformations are characterized by a clustered nidus of vessels with readily identifiable high flow arterial feeders and draining veins. These are

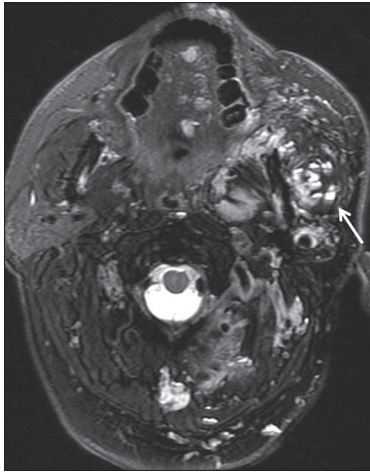


Figure 14: Vascular malformation. A 49-year-old male with a history of “vascular lesion since birth,” although no prior imaging was available. Axial T2-weighted fat-suppressed image demonstrates a transspatial lesion involving the left parotid space, masticator space, oral tongue, and paraspinous soft tissues. Hemorrhage-fluid levels are present within many portions of the lesion (white arrow), compatible with a lymphatic malformation.

best depicted with dynamic conventional, CT, or MR angiography.

CONCLUSION

A variety of neoplastic and nonneoplastic disease processes can occur within salivary gland tissue. It is extremely important to be familiar with their imaging findings, so that a preoperative determination can be made regarding whether a lesion is benign or malignant. Not only can this determine whether surgery is necessary, but it also strongly influences which surgical approach is chosen. In addition, improper characterization of salivary gland lesions can delay diagnosis and, in the case of pleomorphic adenoma, allow time for a benign lesion to undergo malignant transformation. By reviewing the imaging appearance of common neoplastic and tumor-like conditions that can be seen in the salivary glands, we hoped to enhance the imager’s search pattern and improve diagnostic accuracy when approaching a salivary gland mass.

Financial support and sponsorship

Nil.

Conflicts of interest

There are no conflicts of interest.

REFERENCES

- Everson JW, Auclair P, Gnepp DR, El-Naggar AK. Tumors of the salivary glands. In: Barnes L, Eveson JW, Reichart P, Sidransky D, editors. World Health Organization Classification of Tumors. Pathology and Genetics of Head and Neck Tumors. Lyon: IARC Press; 2005. p. 212-5.
- Pinkston JA, Cole P. Incidence rates of salivary gland tumors: Results from a population-based study. *Otolaryngol Head Neck Surg* 1999;120:834-40.
- Lee YY, Wong KT, King AD, Ahuja AT. Imaging of salivary gland tumours. *Eur J Radiol* 2008;66:419-36.
- Christe A, Waldherr C, Hallett R, Zbaeren P, Thoeny H. MR imaging of parotid tumors: Typical lesion characteristics in MR imaging improve discrimination between benign and malignant disease. *AJNR Am J Neuroradiol* 2011;32:1202-7.
- Thoeny HC. Imaging of salivary gland tumours. *Cancer Imaging* 2007;7:52-62.
- Zaghi S, Hendizadeh L, Hung T, Farahvar S, Abemayor E, Sepahdari AR, et al. MRI criteria for the diagnosis of pleomorphic adenoma: A validation study. *Am J Otolaryngol* 2014;35:713-8.
- Valstar MH, de Ridder M, van den Broek EC, Stuijver MM, van Dijk BA, van Velthuysen ML, et al. Salivary gland pleomorphic adenoma in the Netherlands: A nationwide observational study of primary tumor incidence, malignant transformation, recurrence, and risk factors for recurrence. *Oral Oncol* 2017;66:93-9.
- Kato H, Kanematsu M, Mizuta K, Ito Y, Hirose Y. Carcinoma ex pleomorphic adenoma of the parotid gland: Radiologic-pathologic correlation with MR imaging including diffusion-weighted imaging. *AJNR Am J Neuroradiol* 2008;29:865-7.
- Peter Klussmann J, Wittekindt C, Florian Preuss S, Al Attab A, Schroeder U, Guntinas-Lichius O, et al. High risk for bilateral Warthin tumor in heavy smokers – Review of 185 cases. *Acta Otolaryngol* 2006;126:1213-7.
- Ikeda M, Motoori K, Hanazawa T, Nagai Y, Yamamoto S, Ueda T, et al. Warthin tumor of the parotid gland: Diagnostic value of MR imaging with histopathologic correlation. *AJNR Am J Neuroradiol* 2004;25:1256-62.
- Minami M, Tanioka H, Oyama K, Itai Y, Eguchi M, Yoshikawa K, et al. Warthin tumor of the parotid gland: MR-pathologic correlation. *AJNR Am J Neuroradiol* 1993;14:209-14.
- Rapidis AD, Givalos N, Gakiopoulou H, Stavrianos SD, Faratzis G, Lagogiannis GA, et al. Mucoepidermoid carcinoma of the salivary glands. Review of the literature and clinicopathological analysis of 18 patients. *Oral Oncol* 2007;43:130-6.
- Joseph TP, Joseph CP, Jayalakshmy PS, Poothode U. Diagnostic challenges in cytology of mucoepidermoid carcinoma: Report of 6 cases with histopathological correlation. *J Cytol* 2015;32:21-4.
- van Weert S, van der Waal I, Witte BI, Leemans CR, Bloemena E. Histopathological grading of adenoid cystic carcinoma of the head and neck: Analysis of currently used grading systems and proposal for a simplified grading scheme. *Oral Oncol* 2015;51:71-6.
- International Head and Neck Scientific Group. Cervical lymph node metastasis in adenoid cystic carcinoma of the major salivary glands. *J Laryngol Otol* 2017;131:96-105.
- Lewis AG, Tong T, Maghami E. Diagnosis and management of malignant salivary gland tumors of the parotid gland. *Otolaryngol Clin North Am* 2016;49:343-80.
- Som PM, Biller HF. High-grade malignancies of the parotid gland: Identification with MR imaging. *Radiology* 1989;173:823-6.
- Maroldi R, Farina D, Borghesi A, Marconi A, Gatti E. Perineural tumor spread. *Neuroimaging Clin N Am* 2008;18:413-29, xi.
- Andersen LJ, Therkildsen MH, Ockelmann HH, Bentzen JD, Schiødt T, Hansen HS, et al. Malignant epithelial tumors in the minor salivary glands, the submandibular gland, and the sublingual gland. Prognostic factors and treatment results. *Cancer* 1991;68:2431-7.
- Singh FM, Mak SY, Bonington SC. Patterns of spread of head

- and neck adenoid cystic carcinoma. *Clin Radiol* 2015;70:644-53.
21. Li J, Gong X, Xiong P, Xu Q, Liu Y, Chen Y, et al. Ultrasound and computed tomography features of primary acinic cell carcinoma in the parotid gland: A retrospective study. *Eur J Radiol* 2014;83:1152-6.
 22. Al-Zaher N, Obeid A, Al-Salam S, Al-Kayyali BS. Acinic cell carcinoma of the salivary glands: A literature review. *Hematol Oncol Stem Cell Ther* 2009;2:259-64.
 23. Patel ND, van Zante A, Eisele DW, Harnsberger HR, Glastonbury CM. Oncocytoma: The vanishing parotid mass. *AJNR Am J Neuroradiol* 2011;32:1703-6.
 24. Shah VN, Branstetter BF 4th. Oncocytoma of the parotid gland: A potential false-positive finding on 18F-FDG PET. *AJR Am J Roentgenol* 2007;189:W212-4.
 25. Paparo F, Massarelli M, Giuliani G. A rare case of parotid gland lipoma arising from the deep lobe of the parotid gland. *Ann Maxillofac Surg* 2016;6:308-10.
 26. Pandey D, Vats M, Akhtar A, Pathania OP. Sialolipoma of the parotid gland: A rare entity. *BMJ Case Rep* 2015;2015. pii: bcr2014209264.
 27. Clark J, Wang S. Metastatic cancer to the parotid. *Adv Otorhinolaryngol* 2016;78:95-103.
 28. Kashiwagi N, Murakami T, Toguchi M, Nakanishi K, Hidaka S, Fukui H, et al. Metastases to the parotid nodes: CT and MR imaging findings. *Dentomaxillofac Radiol* 2016;45:20160201.
 29. Roebuck DJ, Ahuja AT. Hemangioendothelioma of the parotid gland in infants: Sonography and correlative MR imaging. *AJNR Am J Neuroradiol* 2000;21:219-23.
 30. Tuna İS, Doganay S, Yıkılmaz A, Coskun A. Hemangioma of the parotid gland in an infant: MR and Doppler US findings. *Eurasian J Med* 2009;41:141.
 31. Lara-Sánchez H, Peral-Cagigal B, Madrigal-Rubiales B, Verrier-Hernández A. Cavernous hemangioma of the parotid gland in adults. *J Clin Exp Dent* 2014;6:e592-4.
 32. Coit WE, Harnsberger HR, Osborn AG, Smoker WR, Stevens MH, Lufkin RB, et al. Ranulas and their mimics: CT evaluation. *Radiology* 1987;163:211-6.
 33. Merrow AC, Gupta A, Patel MN, Adams DM. 2014 revised classification of vascular lesions from the international society for the study of vascular anomalies: Radiologic-pathologic update. *Radiographics* 2016;36:1494-516.
 34. Wassef M, Blei F, Adams D, Alomari A, Baselga E, Berenstein A, et al. Vascular anomalies classification: Recommendations from the international society for the study of vascular anomalies. *Pediatrics* 2015;136:e203-14.